nature climate change

SUPPLEMENTARY INFORMATION

DOI: 10.1038/NCLIMATE2357

Climate model simulations of the observed early-2000s hiatus of global warming

Gerald A. Meehl[1], Haiyan Teng[1], and Julie M. Arblaster[1,2]

1. National Center for Atmospheric Research, Boulder, CO

2. CAWCR, Melbourne, Australia

August 21, 2014

Mailing address: Gerald A. Meehl

National Center for Atmospheric Research

3090 Center Green Dr.

Boulder, CO 80301

DOI: 10.1038/NCLIMATE2357

Supplementary Information

The Interdecadal Oscillation (IPO): The IPO[1,2], defined as the second EOF of low-pass filtered observed SSTs for the Pacific region[3] (40°S-60°N, 120°E-80°W, as opposed to the closely related Pacific Decadal Oscillation (PDO)[4] which is defined for SSTs in the North Pacific north of 20°N), is calculated from observed SSTs[5] over the 1870-2012 period and shown in Fig. S1 bottom. The histogram of the pattern correlations between this pattern and the CMIP5 2000-2013 surface temperature trends is plotted in Fig. 2c. For reference, the trend of observed SSTs for the period of the hiatus (2000-2013) from the NOAA OI SSTs[6] is shown in Fig. S1 top, with a statistically significant pattern correlation for the Pacific region used in Fig. 2c of +0.48, and a pattern correlation for central part of the IPO pattern in the Pacific (40°S-40°N, 170°E-80°W) of +0.58.
The results presented in the main text indicate that the early-2000s hiatus and associated negative IPO is being produced mainly by internal variability, with possible smaller contributions to the magnitude of the IPO from the relatively large warming trend in the Indian Ocean[7,8] or the collection of moderate volcanic eruptions since the turn of the century[9].

Bias Adjustment: Models and variables from the CMIP5 decadal prediction experiments that are analyzed in this study are listed in Table S1. Due to model drift caused by initialization, we bias adjust[10] both surface air temperature and zonal wind stress using NCEP/NCAR reanalysis as the observations[11]. For both the observations

and model outputs, annual means are calculated from the monthly outputs and then interpolated to T42 grids, which correspond to approximately a 2.8° latitude/longitude grid spacing. At each grid point, climatological annual mean differences for the ten-year hindcasts are computed with regard to the reanalysis data and composited by year following the start year of all the hindcast simulations. Then these averaged time-evolving annual mean biases are subtracted using cross-validation from each hindcast/prediction. This method may not be optimum for some models[12]. It is chosen here because it is more feasible for multi-model analysis. Since there are no credible observations for net downward heat flux at the ocean surface during the study period, interannual anomalies are calculated from the long-term model climatology[13]. Observations of globally averaged surface temperatures use the HadCRUT4 data[14].

DOI: 10.1038/NCLIMATE2357

Table S1: Summary of CMIP5 models used in the present study[a].

Model	Anomaly assimilation?	# start years	Ensemble size	Surface air temperature	Zonal wind stress	Net downward flux at ocean surface
BCC-CSM1.1	no	15	4/3 [c]	x	x	x
CanCM4 (i1)[b]	no	52	10	x	x	
CanCM4 (i2)	no	17	10	x	x	
CCSM4 (i1)	no	12	10	x	x	x
CCSM4 (i2)	no	15	10	x	x	x
CNRM-CM5	no	20	10	x		
FGOALS-g2	no	7	3	x	x	x
GFDL-CM2p1	no	52	10	x		
HadCM3 (i2)	yes	50	10	x	x	
HadCM3 (i3)	no	50	10	x	x	
IPSL-CM5A-LR	yes	10	6	x	x	
MIROC4h	yes	10	6	x	x	x
MIROC5	yes	52	6	x	x	x
MPI-ESM-LR	yes	51	3/10 [c]	x	x	x
MPI-ESM-MR	yes	19	3	x	x	
MRI-CGCM3	yes	12	3	x	x	x

[a] Decadal predictions from several models (GEOS-5, CMCC-CM, CFSv2-2011, EC-EARTH and FGOALs-s2) are not included in the present analysis due to lack of uninitialized simulations or missing data.

[b] CanCM4, CCSM4 and HadCM3 have applied two different initialization schemes, which are denoted by i1, i2 or i3 consistent with the filenames from PCMDI.

[c] 4/3 = 3 members for all 15 start years and 4 members for 10 start years; 3/10 = 3 members for every start year (10 members for the 5th year)

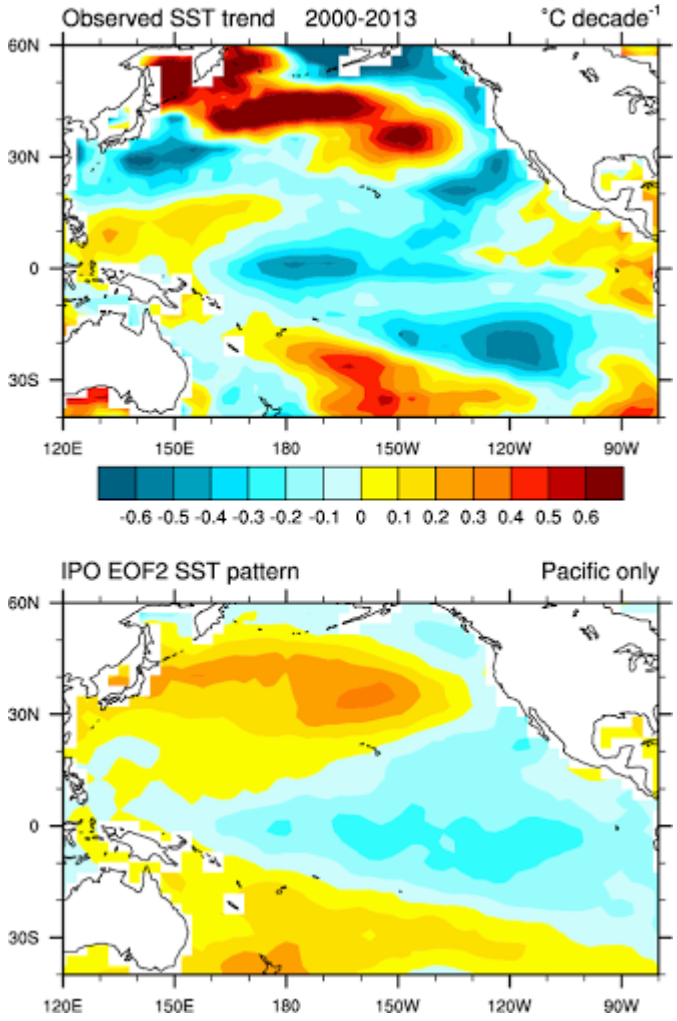

Fig. S1: top: observed NOAA OI SST trend, 2000-2013 (°C/decade); bottom: second EOF of low-pass filtered SSTs computed using only Pacific SSTs from 40°S to 60°N, 120°E-90°W (see Meehl et al. 2009). The IPO pattern is produced by regressing the PC time series onto the SSTs at the grid point level. More observations of the current observed hiatus are also shown in reference 15.

DOI: 10.1038/NCLIMATE2357

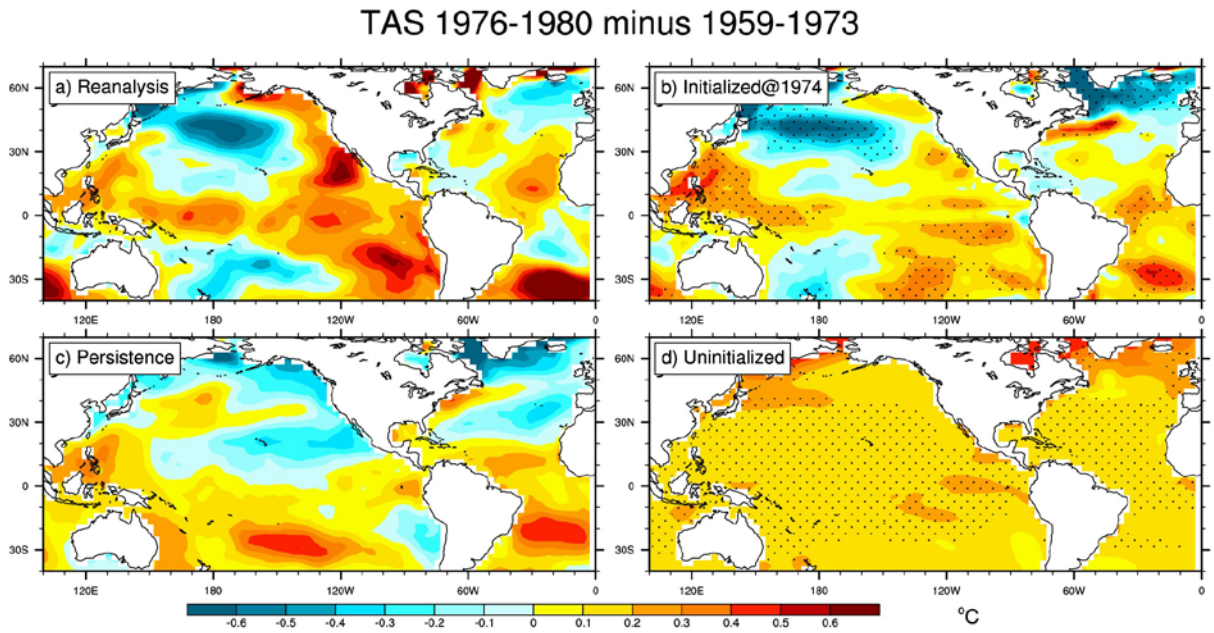

Fig. S2: Surface air temperature patterns for prediction of the IPO transition in the late 1970s; a) Observed sea surface temperature anomalies for 1976-1980 minus 1959-1973; b) 3-7 year hindcast initialized in 1974 for years 1976-1980 minus the observed reference period 1959-1973; c) persistence prediction for years 1976-1980, and d) uninitialized prediction for years 1976-1980 minus the models' reference period 1959-1973. Stippling in panels b and d indicates 10% significance level from a 2-sided t test.

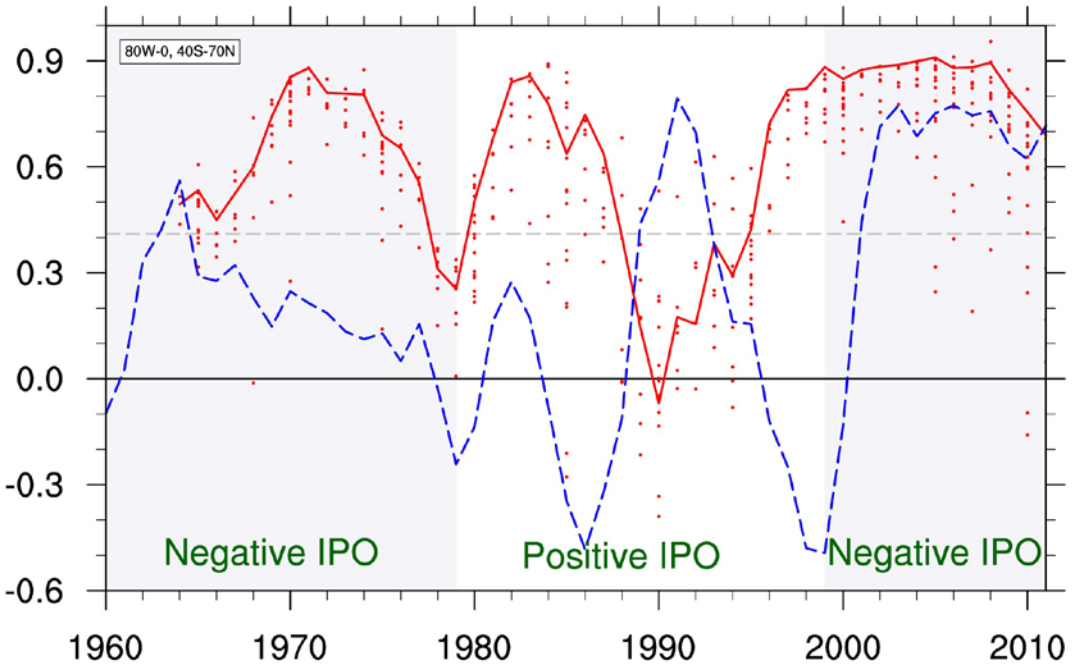

Fig. S3: Anomaly pattern correlations between observations and year 3-7 hindcasts as in Fig. 2e in the main text, but for the Atlantic sector only; individual model values are red dots, multi-model ensemble average is red line, and persistence is dashed blue.

DOI: 10.1038/NCLIMATE2357

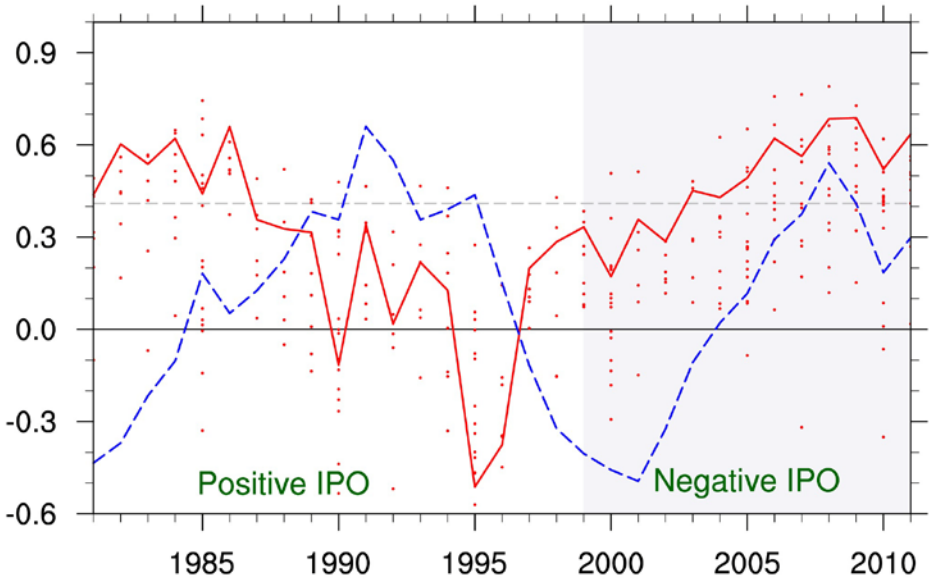

Fig. S4: Anomaly pattern correlations for hindcasts for the Pacific-Atlantic Ocean region (40°S-70°N, 100°E-360°E) surface air temperature, ocean points only, with observed data 1960 through 2011 using the entire hindcast period as climatology from 1960-2011 to document the transition from positive to negative IPO in the late-1990s (red line is multi-model average, red dots are single model results, blue dashed line is persistence prediction, dashed line indicates 95% significance). Compared to Fig. 2d, the somewhat lower pattern correlation values around the time of the transition are partly due to the trend that is introduced in the climatology for this reference period of 1960-2011 that has a similar pattern to that from the greenhouse gas forcing[16].

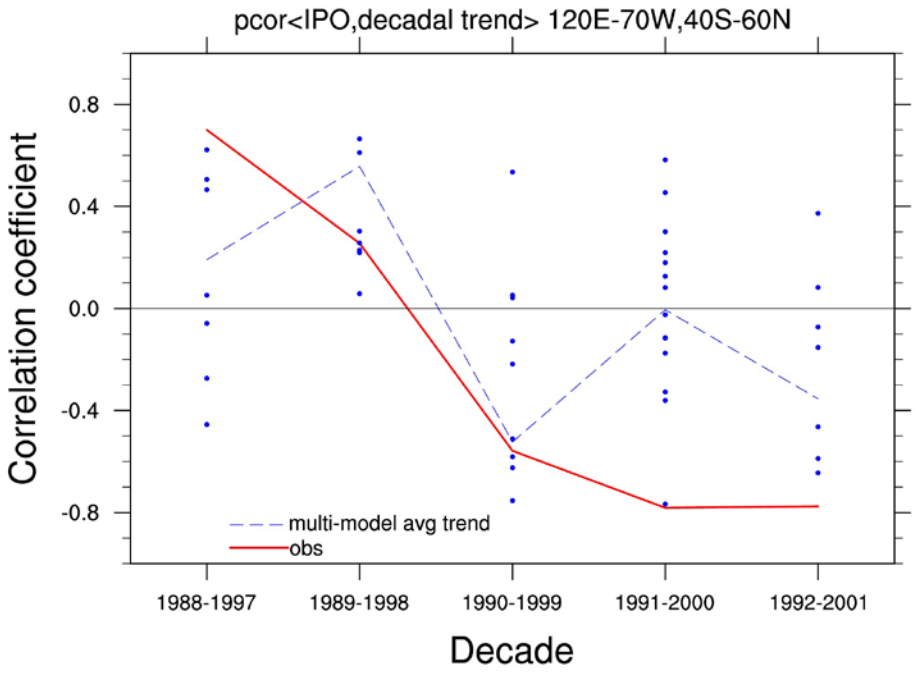

Fig. S5: Anomaly pattern correlations between the observed IPO pattern in Fig. S1b and the decadal SST trends (x axis) for the Pacific region for observations (red line), the multi-model average (dashed blue) and individual models (blue dots) showing that the observed late-1990s transition from positive to negative IPO is simulated by the CMIP5 multi-models using this metric.

DOI: 10.1038/NCLIMATE2357

References in Supplementary Information

1. Power, S. and coauthors, 1999: Interdecadal modulation of the impact of ENSO on Australia. *Clim. Dyn*., **15**, 319-324.

2. Parker, D., C. Folland, A. Scaife, J. Knight, A. Colman, P. Baines, and B. Dong (2007), Decadal to multidecadal variability and the climate change background, J. Geophys. Res., 112, D18115, doi:10.1029/2007JD008411.

3. Meehl, G. A., A. Hu, and B.D. Santer, 2009: The mid-1970s climate shift in the Pacific and the relative roles of forced versus inherent decadal variability, *J. Climate*, **22**, 780--792.

4. Mantua, N.J. and S.R. Hare, Y. Zhang, J.M. Wallace, and R.C. Francis, 1997: A Pacific interdecadal climate oscillation with impacts on salmon production. *Bull. Amer. Meteorol. Soc*., **78**, 1069-1079.

5. Hurrell J.W., J.J. Hack, D. Shea, J.M. Caron, and J. Rosinski, 2008: A New Sea Surface Temperature and Sea Ice Boundary Dataset for the Community Atmosphere Model, *J. Climate*, **21**, 5145-5153, doi:10.1175/2008JCLI2292.1.

6. Reynolds, R.W., N.A. Rayner, T.M. Smith, D.C. Stokes, and W. Wang, 2002: An improved in situ and satellite SST analysis for climate, *J. Climate,*, **15**, 1609-1625.

7. Luo, J.-J., W. Sasaki, and Y. Masumoto, 2012: Indian Ocean warming modulates Pacific climate change. *PNAS*, 109, 18701-18706, doi:10.1073/pnas.1210239109

8. Han, W., and co-authors, 2013: Intensification of decadal and multi-decadal sea level variability in the western tropical Pacific during recent decades. *Clim. Dyn.*, doi:10.1007/s00382-013-1951-1.

9. Santer, B.D., et al., 2014: Volcanic contribution to decadal changes in tropospheric temperature. *Nature Geoscience*, 7, 185-189, doi:10.1038/ngeo2089.

10. CLIVAR (2011), Data and bias correction for decadal climate prediction. CLIVAR Publication Series 150, International CLIVAR Project Office, 4pp.

11. Kalnay, E. and coauthors (1996), The NCEP/NCAR 40-year Reanalysis Project. *Bull. Amer. Meteorol. Soc.*, *77*, 437-471.

12. Meehl, G.A., and H. Teng, 2014: CMIP5 multi-model initialized decadal hindcasts for the mid-1970s shift and early-2000s hiatus and predictions for 2016-2035. *Geophys. Res. Lett*., doi:10.1002/2014GL059256.

13. Guemas, V., F.J. Doblas-Reyes, I. Andreu-Burillo, and M. Asif (2013), Retrospective prediction of the global warming slowdown in the past decade. *Nature Climate Change*, 3, 649-653, doi:10.1038/nclimate1863.

DOI: 10.1038/NCLIMATE2357

14. Morice, C.P., Kennedy, J.J., Rayner, N.A. and Jones, P.D., 2012: Quantifying uncertainties in global and regional temperature change using an ensemble of observational estimates: the HadCRUT4 dataset. *Journal of Geophysical Research*, **117**, D08101, doi:10.1029/2011JD017187.

15. Trenberth, K.E. and co-authors, Seasonal aspects of the recent pause in surface warming, *Nature Climate Change*, submitted.

16. Meehl, G. A., A. Hu, and B.D. Santer, 2009: The mid-1970s climate shift in the Pacific and the relative roles of forced versus inherent decadal variability, *J. Climate*, **22**, 780--792.